

## Research Article

## Open Access

Lidao Bao, Yi Wang, Ruilian Ma, Xianhua Ren, Haijun Lv\*, Agula B

# Effect of puerarin on human choriocarcinoma cells

**Abstract:** Objective: To discuss the effect of puerarin on human choriocarcinoma cells. Methods: Survival rates under puerarin monotherapy, fluorouracil (5-FU) monotherapy and puerarin in combination with 5-FU were detected by MTT assay. Apoptotic morphology was observed with Hoechst 33258 staining. Apoptosis rates were detected with flow cytometry. Expressions of AKT, mechanistic target of rapamycin (mTOR), and P70S6K mRNAs and phosphorylated proteins were detected by RT-PCR and Western blot. Tumor-bearing mice were administered puerarin and puerarin+5-FU, and serum levels of  $\beta$ -human chorionic gonadotropin ( $\beta$ -HCG) were measured. Results: Proliferation inhibition and apoptosis rates of JEG-3 cells were positively correlated with puerarin concentration, which increased in the puerarin+5-FU group. Expression levels of AKT, mTOR, P70S6K mRNAs, and phosphorylated proteins decreased significantly after action of puerarin at different concentrations. With increasing puerarin concentration, expression of cleaved-caspase-3 in JEG-3 cells increased, whereas that of Bcl-2 decreased. Puerarin significantly inhibited tumor growth in choriocarcinoma-bearing SCID mice. Serum  $\beta$ -HCG levels were significantly lower than those of control group after administration. Magnitude of  $\beta$ -HCG decline was positively correlated with concentration.. Conclusion: Puerarin+5-FU inhibited proliferation of JEG-3 choriocarcinoma cells and promoted their apoptosis, being associated with the mTOR signaling pathway.

**Keywords:** puerarin, fluorouracil, JEG-3, choriocarcinoma

DOI 10.1515/med-2015-0039

Received January 31, 2015; accepted March 19, 2015

**\*Corresponding author: Haijun Lv:** Department of Scientific Research, Affiliated Hospital of Inner Mongolia Medical University, Hohhot 010059, PR China, E-mail: lvhaijundsr@163.com  
**Lidao Bao, Yi Wang, Ruilian Ma, Xianhua Ren:** Department of Pharmacy, Affiliated Hospital of Inner Mongolia Medical University, Hohhot 010059, PR China  
**Agula B:** College of Mongolian Medicine, Inner Mongolia Medical University, Hohhot 010059, PR China

## 1 Introduction

Choriocarcinoma, a malignant tumor that originates from embryonic trophocytes, tends to occur in women of childbearing age [1,2]. It invades the myometrium or metastasizes to other organs, thus causing damage and death because that the trophocytes will lose their villi following malignant transformation. Currently in China, the most commonly used drugs are fluorouracil (5-FU) and dactinomycin [3]. As we cannot totally solve the problems of choriocarcinoma drug resistance, relapse, and toxic and side effects of chemotherapy drugs [4,5] at present, we need to seek new effective low-toxicity antineoplastic drugs and to explore the molecular mechanism of the drugs, thereby making it possible to effectively administer targeted therapy. Extensive and profound Chinese medical science shows great potential in development of new drugs [6,7]. Antineoplastic drugs extracted from the natural traditional Chinese medicines have rich sources and few toxic side effects. In recent years, the experts both at home and abroad have conducted cell experiments using traditional Chinese medicines and their effective extractive preparations [8]. It has been discovered that inducing thereby tumor cell apoptosis, Chinese herbs can regulate oncogenes in a multi-factorial and multi-level manner: it can affect gene expression and influence the expression level of the regulator gene, thus achieving the antineoplastic effect.

Radix Puerariae, a common drug in China, is widely distributed in various regions of that country, with the exception of Xinjiang, Qinghai, and Tibet. Puerarin (HPLC) is prepared by extraction of Radix Puerariae. The main dosage forms include tablet and injectionables. The main chemical constituents are a flavonoid compound and pueraria flavones. This drug can, for example, improve immunity, strengthen myocardial contractility, protect myocardial cells, reduce blood pressure, and inhibit platelet aggregation. The flavonoid compounds play a role in inhibiting initiation, promotion, and development of the carcinogenic process as a result of their antioxidant activity and capacity to absorb UV light. Hence, puerarin has long been used for treatment of cancers, but there is little research on the mechanism

of the its antineoplastic effect [7,9]. The mechanistic target of rapamycin (mTOR) signaling pathway is one of the signal transduction pathways [10,11] intimately associated with cell differentiation and proliferation. In this way, it plays an important role in synthesizing tumor cell proteins, regulating cell cycle-related protein, and adjusting tumor angiogenesis. Currently, there is little research on choriocarcinoma and mTOR signaling. Most of the research involves gestational trophocytes and choriocarcinoma cell strains, with a focus on other aspects. However, there has been evidence that suggests activation of the mTOR signaling pathway in choriocarcinoma. Some scholars have extracted puerarin, a monomeric compound, from the Kudzu root [9]. Animal experiments have demonstrated that it has few toxic side effects. The preliminary result has indicated that the toxic dose in rats is 1000 mg/kg. To explore whether puerarin has an antineoplastic effect on human choriocarcinoma, we first observed the effect of puerarin on proliferation and apoptosis of human choriocarcinoma JEG-3 cells, and further, observed its efficacy, toxicity, side effects in animal models, and preliminarily discussed the mechanism of its antineoplastic effect on choriocarcinoma cells and its relationship with the mTOR signaling pathway.

## 2 Materials and Methods

All experiments were performed in compliance with the relevant laws and/or institutional guidelines of Affiliated Hospital of Inner Mongolia Medical University.

### 2.1 Source of cells

Human choriocarcinoma JEG-3 cell strains were purchased from Laboratory of Birth Control and Reproductive Biology, Institute of Zoology, Inner Mongolia Medical University.

### 2.2 Experimental animals

Female SCID mice (Shanghai Slac Laboratory Animal Co., Ltd.) aged 4-5 weeks, weighing  $15 \pm 0.26$  g, were raised under specific pathogen-free conditions at a constant temperature (18-22°C) and a constant humidity (50-80%).

### 2.3 Main reagents and instruments

The main reagents and instruments included: puerarin (purified in the laboratory), 5-FU (Donghaipu Pharmacy, Shanghai), culture media (RPMI 1640) (U.S. Hyclon Company), dimethylsulfoxide (DMSO), trypsin (U.S.

Amersco Company), MTT (U.S. Sigma Company), fetal bovine serum (Hangzhou Sijiqing Bio-engineering Material Co., Ltd.), mouse anti-human Akt, mTOR, p70S6K, Bcl-2, caspase-3, phosphorylated anti-Akt (Ser473), anti-mTOR (Ser2448), and anti-p70S6K (Thr389) (U.S. CST Company), PCR primers (Shanghai Sangon Biotech Co., Ltd.), reverse transcription kits (U.S. Fermentas Company), cell incubators (Sweden NUNER Company), an inverted microscope (Australia LEICA Company), a fluorescence microscope (Japan Olympus Company), PCR amplifier (Germany Eppendorf Company), and an electrophoresis apparatus, a membrane transfer device (U.S. BIO-RAD Company).

### 2.4 Cell culture

Human choriocarcinoma JEG-3 cells were grown in RPMI 1640 culture medium containing 10% fetal bovine serum (Hangzhou Sijiqing Bio-engineering Material Co., Ltd.), double-antibody (20000 U/mL penicillin (Shijiazhuang Huabei Pharmacy), 20000 mg/mL streptomycin (Shijiazhuang Huabei Pharmacy)), 200 nM glutamine (Shijiazhuang Huabei Pharmacy), and 50 mM sodium pyruvate (Shijiazhuang Huabei Pharmacy), cultured at 37°C, in an environment containing 5% CO<sub>2</sub> with saturation humidity, with the culture medium replaced once every 48-72 h, passaged as per 1:3 [12].

### 2.5 Detecting cell proliferation (MTT method) with cell proliferation inhibition experiment

Puerarin group: Puerarin of different mass concentrations (0.1, 0.5, 1.0, 5.0, 10.0, 20.0, and 50.0  $\mu\text{mol/L}$ ) was used to treat the JEG-3 cells for 24, 48, and 72 h. Treatment groups were defined as follows. In the 5-FU Group, 5-FU of different mass concentrations (2.5, 5.0, 10.0, 25.0, 50.0, 100.0, and 200.0  $\mu\text{g/ml}$ ) was used to treat the JEG-3 cells for 48 h; in the puerarin+5-FU group, puerarin at a final concentration of 5  $\mu\text{mol/L}$  was bathed with 5-FU of different concentrations for 48 h; and in the control group, no drugs were added to the JEG-3 cells for intervention and only the culture medium containing menstuum (0.1% DMSO) was added [13].

The JEG-3 cells in the logarithmic phase were collected for preparation of cell suspension. The cell suspension was cultured for 24 h until the cell fusion degree reached approximately 80%. Culture medium (200  $\mu\text{L}$ ) containing drugs at corresponding concentrations was added to all experimental groups; the culture medium containing the dissolved drug was added to the control group. It was

cultured for 4 h after addition of 10  $\mu$ L 0.5% MTT with a micropipette 4 h after termination of the drug action. The supernatant was discarded. DMSO (200  $\mu$ L) was added to each well. The cells were cultured at 37°C for 30 min. The absorbance value of each well was detected at 570 nm by an enzyme-linked immunosorbent assay (ELISA) microplate reader; each microplate was detected 3 times to calculate the proliferation inhibition rate: proliferation Inhibition Rate (IR)% = (1-OD administration/OD control) $\times$ 100% (OD: optical density).

## 2.6 Observation of morphology of apoptotic cells

The JEG-3 cells in the logarithmic phase were collected [14] to prepare a cell suspension at a concentration of  $1\times 10^6$ /mL. The cell suspension was added to a 6-well microplate with 1 mL for each well, cultured at 37°C for 24 h, incubated for 48 h in a medium of different concentration, washed twice with PBS, stained for 10 min away from light after addition of 5  $\mu$ g/mL Hoechst 33258. The cells were observed for apoptosis under ultraviolet light with a fluorescence microscope.

After all groups were subjected to drug intervention, the cells of the logarithmic phase were collected to prepare a cell suspension at a concentration of  $1\times 10^6$ /mL, inoculated into a 6-well microplate with 1 mL for each well, cultured for 72 h at 37°C in an environment containing 5% CO<sub>2</sub>, digested with 5% pancreatin, and washed twice with PBS after the supernatant was discarded. The cells (100  $\mu$ L) were suspended in a 1.5 mL PE tube after the cell concentration was adjusted to  $1\times 10^6$ /mL. Operations were carried out in accordance with the instructions for the Annexin V/PI double-staining kit. The cells were re-suspended in 400  $\mu$ L PBS after reacting for 15 min at room temperature away from light, screened with 1 300-mesh sieve, transferred to a flow tube, and detected for apoptosis with a flow cytometer. Excitation wavelength Ex=488 nm; emission wavelength Em=530 nm.

## 2.7 Detecting expression of genes in cells in various groups with RT-PCR

The drug treatment was the same as that in section 1.6; 1 mL of TRIzol lysis buffer was added to extract the total RNA. The total RNA of cells was obtained after precipitating with isopropanol. RNA (2  $\mu$ L) was observed under the gel imaging system following electrophoresis. The cDNA was reverse transcribed, with the total mRNA of cells being the template. The target genes were amplified with the gradient PCR technique. The upstream and downstream

primers were designed using the Primer Premier 5.0 software in accordance with the cDNA expression sequence and relevant data provided corresponding to AKT, mTOR, and p70S6K in GenBank [15].

AKT:

A-1: GGGCACTTTCGGCAAGGTGA

A-2: CATGGTGGCACCGTCCTTGA

mTOR:

M-1: AGTGGACCAGTGAAACAGG

M-2: TTCAGCGATGTCTTGTGAGG

p70S6K:

P70-1: TGGTCCTGGGGACGCTGGAG

P70-2: TGCCGAT(jcttccccactca

The amplification products were electrophoresed on 1% agarose gel and observed under the gel imaging system.

## 2.8 Western blotting analysis

Western blot was used to detect the expression of AKT, mTOR, P70S6K, and corresponding phosphorylated proteins and expression of apoptosis-related proteins in various groups [16]. The cells were subject to lysis on ice after suspension. The protein concentration was determined in accordance with the instructions for the BCA protein quantification kit (Shanghai Wei Feng Biotechnology Co., Ltd.). After electrophoretic separation, the protein was transferred onto a PVD membrane, blocked, and subject to reaction with the primary antibodies (anti-Akt (Ser473), anti-mTOR (Ser2448), and anti-p70S (U.S. CST Company)) for 2 h, incubated and developed after addition of the secondary antibody (HRP goat anti-rabbit IgG (U.S. Proteintech Company)).

## 2.9 Animal experiments

The SCID mice (Shanghai Slac Laboratory Animal Co., Ltd.) were randomly divided into 6 groups of 6 each. JEG-3 cell suspension (0.2 mL) was inoculated into the right dorsum of each SCID mouse. Each tumor was inoculated with  $5\times 10^6$  cells. The incubation period of the transplanted tumor was 9–10 days. Intraperitoneal injections were administered once per day after the tumor size reached approximately 50 mm<sup>3</sup>. Four groups were set up: Group 1, control group, no dosage; Group 2, puerarin 20 mg/kg; Group 3, VB 140 mg/kg; Group 4, puerarin 80 mg/kg; Group 5, 5-FU 25 mg/kg; Group 6: puerarin 20 mg/kg+5-FU 25 mg/kg. The transplanted tumor was observed and measured. At 14 d after administration, the complete tumor tissue was separated for measuring and calculating the tumor inhibition rate. The dissected transplanted

tumor tissue was fixed for 7 days at room temperature, dehydrated, sectioned, and baked at 45°C for 24 h. The 4- $\mu\text{m}$ -thick slides were regularly HE stained and observed under a light microscope. The 10- $\mu\text{m}$ -thick slides were baked for 20 min at 68°C, dewaxed, dehydrated, blocked after antigen retrieval, treated with the primary antibody (mouse anti-human p-I-ICG monoclonal antibody working solution for 12 h, PBS substituted for the primary antibody as the negative control), incubated, and developed after addition of the secondary antibody (HRP goat anti-rabbit IgG) (U.S. Proteintech Company). Whole blood was taken through the eye sockets of the SCID mice and centrifuged at 3000 rpm for 5 min. The blood  $\beta$ -human chorionic gonadotropin ( $\beta$ -HCG) of SCID mice was determined with the chemiluminescence method after collection of the serum [17].

## 2.10 Statistical analysis

SPSS 17.0 software was used for statistical analysis; the experimental data were expressed with mean  $\pm$  standard deviation ( $\bar{x} \pm s$ ). The differences in cell proliferation and apoptosis within each group and among various groups were subject to one-way analysis of variance and the Student's *t* test. Differences were considered statistically significant at  $P < 0.05$ .  $IC_{50}$  was calculated based on Probit regression analysis. The gene expression and protein expression used the Quality One software for image gray analysis. The differences within each group and among various groups were subject to one-way analysis of variance and least significant difference-*t* test. The comparisons among various groups were subject to one-way analysis of variance in the experiment. The immunohistochemical results were subject to a non-parametric rank sum test.

## 3 Results

### 3.1 Effect of puerarin on in vitro proliferation of cells

Puerarin of different mass concentrations played a role in inhibiting the in vitro proliferation of the JEG-3 cells and exhibited significant dose dependence. The JEG-3 cell inhibition rate increased significantly with time (24, 48, and 72 h) under the same puerarin action concentration (Table 1).

Figure 1 shows the proliferation inhibition in various groups at 48 h after the action of 5-FU alone at different concentrations and the combined action of 5-FU and 5  $\mu\text{mol/L}$  puerarin. The proliferation inhibition rate for the JEG-3 in the 5-FU monotherapy group increased significantly compared with that in the control group, and the action was positively correlated with the concentration. The proliferation inhibition rate was  $40.26 \pm 0.73\%$  at 48 h after monotherapy when the puerarin concentration was 5  $\mu\text{mol/L}$ . The proliferation inhibition rates in various groups were significantly higher than that in the puerarin monotherapy group, and the inhibition effect was strengthened with the increase of 5-FU concentration when puerarin of the same concentration was used in combination with 5-FU of different concentrations. Compared with the group of 5-FU at the same concentration, the proliferation inhibition rate in the puerarin+5-FU group also increased significantly.

### 3.2 Effect of puerarin on apoptosis of JEG-3 cells

There were changes in morphology of JEG-3 cell nuclei under the action of drug at different concentrations (Figure 2). Normal cells were stained light and uniformly,

**Table 1.** Proliferation inhibition rate for JEG-3 cells under action of puerarin at different concentrations (%).

Puerarin Concentration ( $\mu\text{mol/L}$ )	Action Time (h)		
	24	48	72
Control Group	0.00	0.00	0.00
0.1	$0.63 \pm 0.38^*$	$0.81 \pm 0.45^{*#}$	$4.89 \pm 1.56^{*##}$
0.5	$2.68 \pm 0.49^*$	$8.57 \pm 0.96^{*#}$	$19.56 \pm 1.74^{*##}$
1.0	$11.23 \pm 1.28^*$	$14.45 \pm 1.09^{*#}$	$38.17 \pm 1.93^{*##}$
5.0	$24.19 \pm 1.06^*$	$40.26 \pm 0.73^{*#}$	$69.34 \pm 0.82^{*##}$
10.0	$37.22 \pm 0.52^*$	$70.84 \pm 0.40^{*#}$	$74.88 \pm 0.35^{*##}$
20.0	$61.58 \pm 0.56^*$	$75.64 \pm 0.23^{*#}$	$82.38 \pm 0.53^{*##}$
50.0	$69.80 \pm 0.73^*$	$81.28 \pm 0.20^{*#}$	$90.38 \pm 0.19^{*##}$

\*Compared with the control group and the previous concentration,  $P < 0.05$ ; #compared with that in the previous period at the same concentration,  $P < 0.05$ .

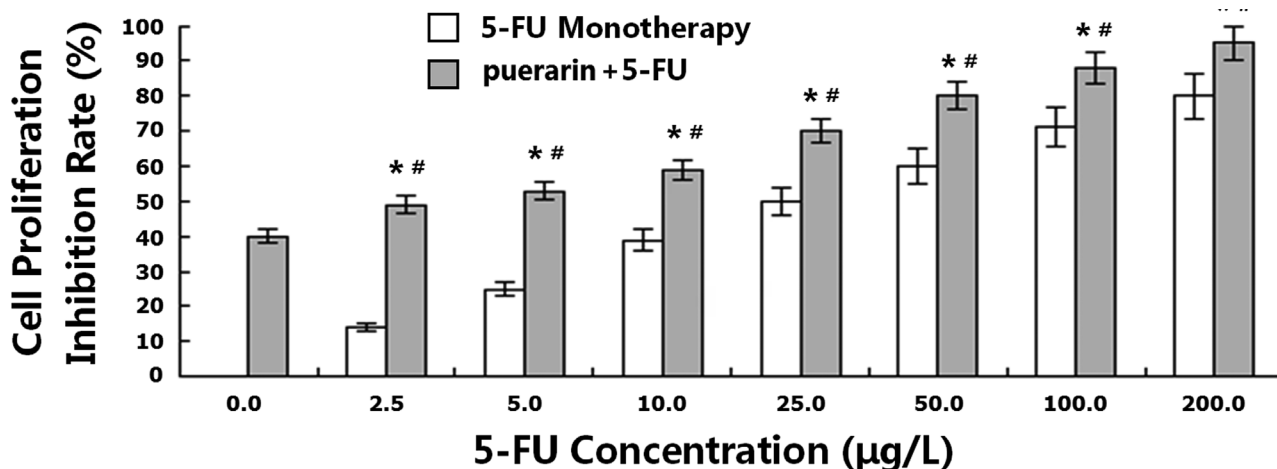


**Figure 1.** Comparison between 5-FU monotherapy and combination of puerarin+5-FU. The proliferation inhibition rate for cells at 48 h after the action of 5.0 µmol/L puerarin alone (5-FU concentration was 0); \* signifies  $P < 0.05$  compared with the puerarin group at 48 h after the action of the 5.0 µmol/L puerarin alone; # signifies  $P < 0.05$  compared with the group of 5-FU at the same concentration.

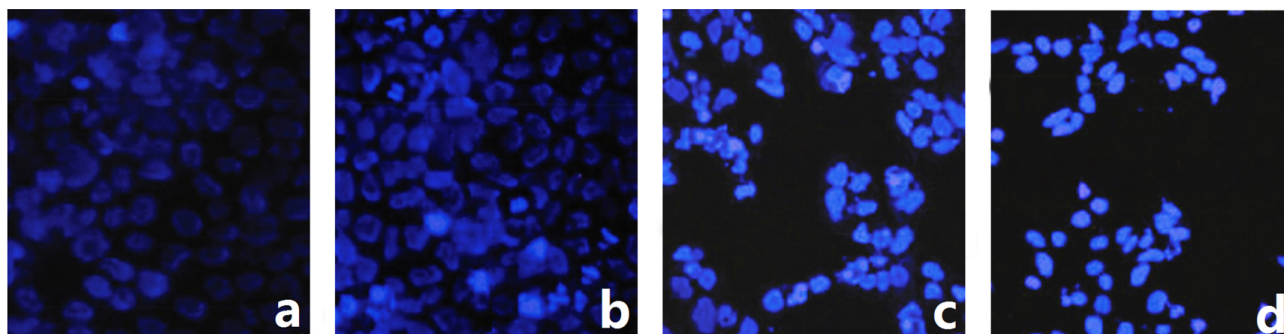


**Figure 2.** Morphological changes of JEG-3 cell nuclei at 48 h following treatment by the drug at different concentrations (fluorescence microscope,  $\times 400$ ). a. control cells: The cell nuclei were stained blue uniformly; b-d, cells treated with puerarin (1, 5, 20 µmol/L L in sequence): The cell nuclei became smaller and brighter to different extents; some nuclei were dissolved and fragmented; apoptosis bodies formed; the higher the concentration was, the more significant the changes in cell apoptosis would be.

whereas the apoptotic cell nuclei were not stained uniformly. The chromatin became concentrated, thus leading to small and bright cell nuclei. Under the fluorescence microscope, the cell apoptosis degree and the drug action concentration were positively correlated; the cell apoptosis was aggravated by the high concentration of drug; there was a large amount of necrotic debris.

The flow cytometer was used to detect cell apoptosis. Figure 3 shows the apoptosis in various groups, indicating that the cell apoptosis rate in each group was significant higher than that in the control group. When puerarin alone was used to treat the JEG-3 cells, the apoptosis rate was positively correlated with the drug concentration. The apoptosis rate in the group with drug combination of puerarin (5 µmol/L) and 5-FU (25 µg/L) increased significantly compared with that in the group with monotherapy at the same concentration (Figure 4).s

### 3.3 Detecting the expression of mRNA in AKT, mTOR, and P70S6K in various groups with RT-PCR

The relative expression of AKT after the JEG-3 cells were treated with puerarin at different concentrations decreased significantly compared with that in the control group; the relative expression of mRNA in mTOR and P70S6K in the 5 µmol/L and 20 µmol/L puerarin groups decreased significantly compared with that in the control group; the relative expression of mRNA in AKT, mTOR, and P70S6K in the 20 µmol/L puerarin group decreased significantly compared with that in the puerarin group at the previous concentration; the difference was significant; various groups exhibited a dose-dependent relationship to some extent (Figure 5A).

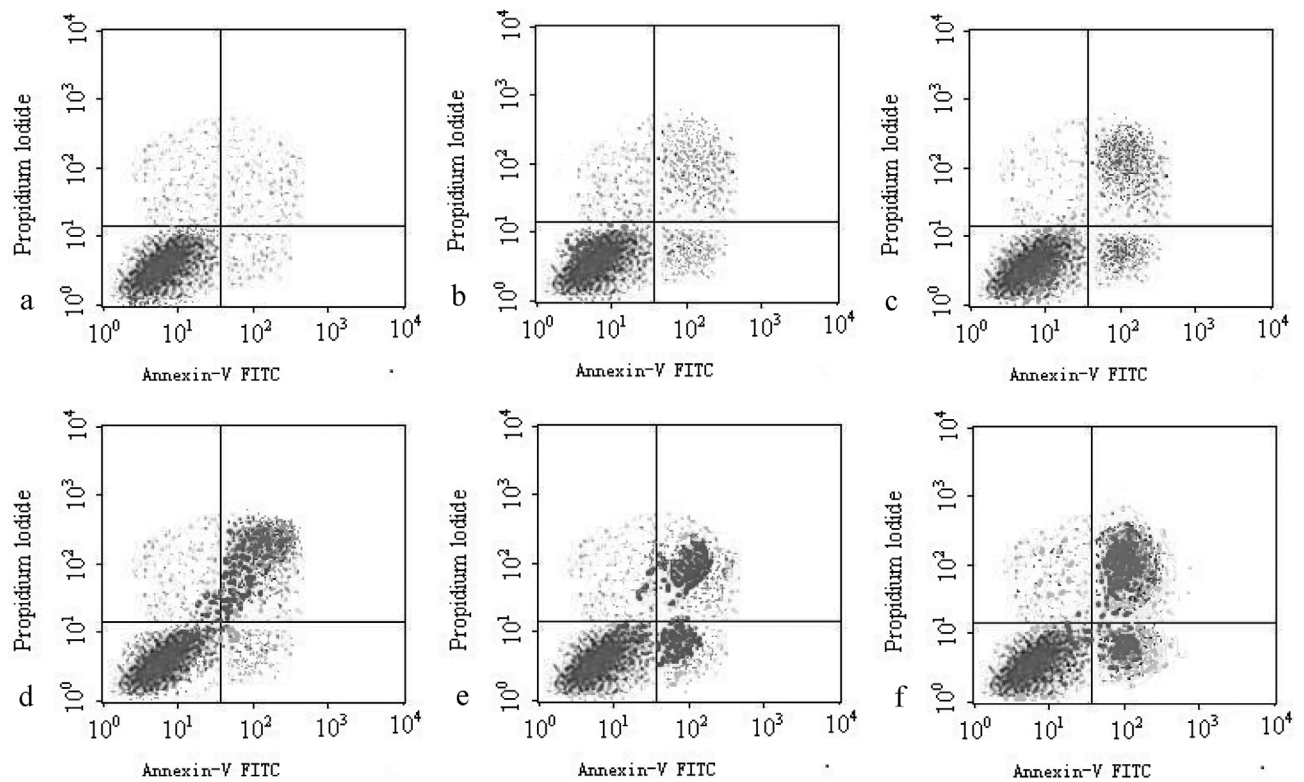


**Figure 3.** Apoptosis in various groups: a is the control group; b is the 1  $\mu\text{mol/L}$  puerarin group; c is the 5  $\mu\text{mol/L}$  puerarin group; d is the 20  $\mu\text{mol/L}$  puerarin group; e is the 25  $\mu\text{g/L}$  5-FU group; f is the 5  $\mu\text{mol/L}$  puerarin+25  $\mu\text{g/L}$  5-FU group.

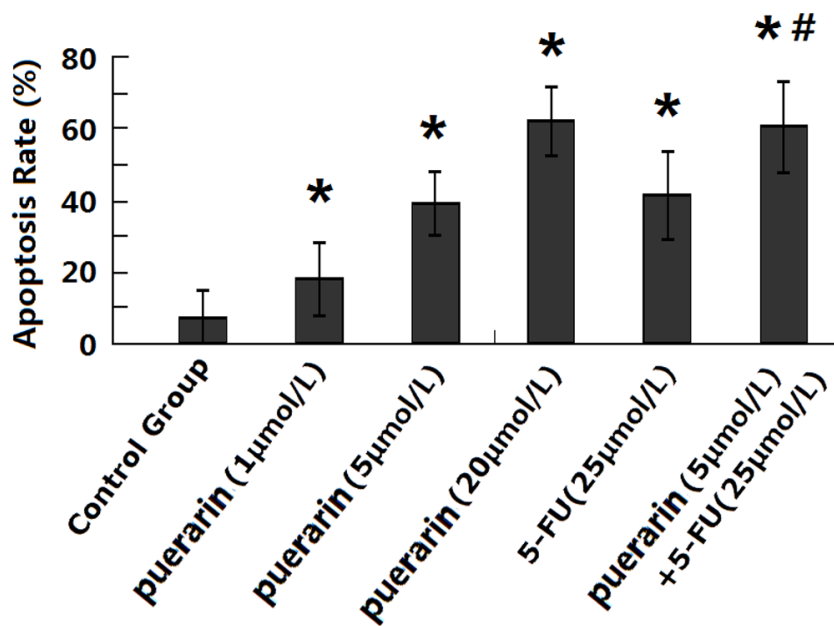


**Figure 4.** Comparison of apoptosis rates in various groups. \* Signifies a significant difference compared with the control group; # signifies that the difference was significant compared with monotherapy at the same concentration..

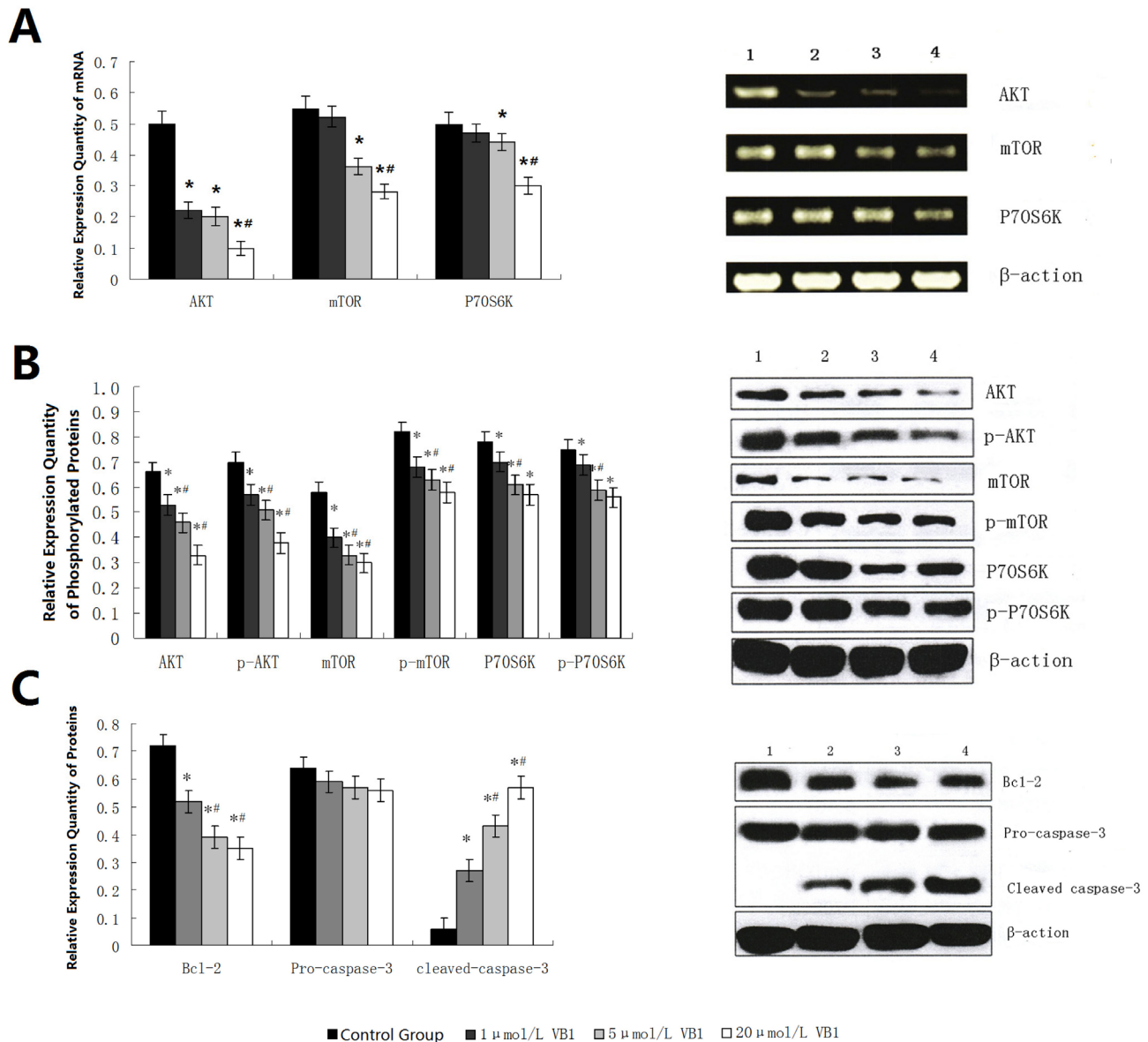


**Figure 5.** A: Expression and relative expression quantities of mRNA in AKT, mTOR, and P70S6K of the cells in different drug treatment groups. The diagram on the left presents the comparisons of relative expression quantities of mRNA in AKT, mTOR, and P70S6K. B: Expression of AKT, mTOR, P70S6K, and corresponding phosphorylated proteins in various groups treated with puerarin at different concentrations. C: Expression of apoptosis-related proteins in various groups treated with puerarin at different concentrations. \* Signifies  $P < 0.05$  compared with the control group; # signifies  $P < 0.05$  compared with the group treated with puerarin at the previous concentration. In the diagram on the right: 1 is the control group, 2 is the 1  $\mu$ mol/L puerarin group, 3 is the 5  $\mu$ mol/L puerarin group, and 4 is the 20  $\mu$ mol/L puerarin group.

### 3.4 Detecting the expression of the AKT, mTOR, P70S6K, and corresponding phosphorylated proteins in various groups with Western blot

The Western blot result indicated that with the rise of the puerarin concentration (Figure 5B) the relative expression quantities of AKT, mTOR, P70S6K, and corresponding phosphorylated proteins in the JEG-3 cells decreased significantly compared with those in the control group; the

relative expression quantities of AKT, mTOR, P70S6K, and corresponding phosphorylated proteins in the 5  $\mu$ mol/L puerarin group and 20  $\mu$ mol/L puerarin group decreased significantly compared with those in the group treated with puerarin at the previous concentration; and the relative expression quantities of P70S6K and corresponding phosphorylated proteins in the 5  $\mu$ mol/L puerarin group decreased significantly compared with those in the group treated with puerarin at the previous concentration. The relative expression quantities of P70S6K and corresponding phosphorylated proteins in the 20  $\mu$ mol/L puerarin group

decreased compared with those in the 5  $\mu\text{mol/L}$  puerarin group, but the difference was not significant.

### 3.5 Detecting expression of the apoptosis-related proteins in various groups treated with puerarin at different concentrations with Western blot

The Western blot result indicated that with the increase of the action concentration of puerarin, the expression of pro-caspase-3 in the JEG-3 cells did not change significantly, whereas the expression of cleaved-caspase-3 increased gradually and the expression of Bcl-2 decreased gradually. The difference was significant compared with the control group. The difference was also significant compared with the group treated with puerarin at the previous concentration, as shown in Figure 5C.

## 3.6 Results of Animal experiments

### 3.6.1 Tumor inhibition rates in various drug groups

The final volume and weight in various groups at the end of the experiment are shown in Table 2. There were significant differences in volume and weight of transplanted tumor between various drug groups and the control group. The tumor volume inhibition rate and tumor weight inhibition rate were positively correlated with the drug concentration. The tumor volume inhibition rate in the high-concentration puerarin group (80 mg/kg) was 75.31%, and the tumor weight inhibition rate was 72.20%. The tumor inhibition rate in the 5-FU monotherapy group (25 mg/kg) was 77.19%, and the tumor weight inhibition rate was 73.54%. The tumor volume inhibition rate and tumor weight inhibition rate in the combination drug therapy group were significantly higher than those in the monotherapy group at the same dose.

### 3.6.2 HE staining result for transplanted tumor tissue

The result indicated that all groups were morphologically similar. There were a large number of highly proliferated heteromorphic trophocytes and syncytial trophocytes. The nested trophocytes were encysted by syncytial trophocytes. There were gaps among cell nests. Well-grown blood vessels were present in the tumor tissue. Hemorrhagic necrosis was present in the tissue. Apoptotic bodies and tumor giant cells were sometimes present. The tumor cells had a large volume and obvious nucleoli (2–3), but had no villi. Nuclear fission was common. The trophocytes cytoplasm was loose, and the karyosome was uniformly distributed in a reticular form. The syncytial trophocytes' cytoplasm was homogeneous and vacuole-shaped; the karyosome was coarse and deep. The proportion of the proliferous trophocytes was different from that of the syncytial trophocytes. Some proliferous trophocytes were disorderly. Degenerative necrosis of oncocytes in the high-dosage puerarin group and the combination drug therapy group was more significant than that in the negative control group (Figure 6A).

### 3.6.3 Immunohistochemical examination results for $\beta$ -HCG protein in the transplanted tumor

The  $\beta$ -HCG protein was in the form of brown particles after immunohistochemical staining. There were a number of such positive cells in the tissue of the transplanted tumor. The brown particles were mainly distributed around the trophocyte nests, mainly concentrated in the tumor cells in the syncytial trophoblast. We observed that the positive particles concentrated in the cytoplasm. Positive particles were also distributed at the bleeding site of the tumor tissue. The immunohistochemical result indicated that the expression of the  $\beta$ -HCG protein in various slides ranged

**Table 2.** Tumor inhibition rates in different drug groups at the end of experiments.

Group	Volume ( $\text{mm}^3$ )	Tumor Volume Inhibition Rate (%)	Weight (g)	Tumor Weight Inhibition Rate
Control Group	4331.08 $\pm$ 157.35		2.23 $\pm$ 0.33	
Puerarin (20 mg/kg)	2362.36 $\pm$ 143.73*	45.46	1.26 $\pm$ 0.21*	43.50
Puerarin (40 mg/kg)	1698.19 $\pm$ 126.56*	60.79	0.89 $\pm$ 0.14*	60.09
Puerarin (80 mg/kg)	1069.36 $\pm$ 78.66*	75.31	0.62 $\pm$ 0.08*	72.20
5-FU (25 mg/kg)	988.13 $\pm$ 68.28*	77.19	0.59 $\pm$ 0.09*	73.54
Puerarin (20 mg/kg)+5-FU (25 mg/kg)	486.45 $\pm$ 79.78*#	88.77	0.31 $\pm$ 0.13*#	86.10

\* Signifies that the difference was significant compared with the control group,; # signifies that the difference was significant compared with monotherapy group.



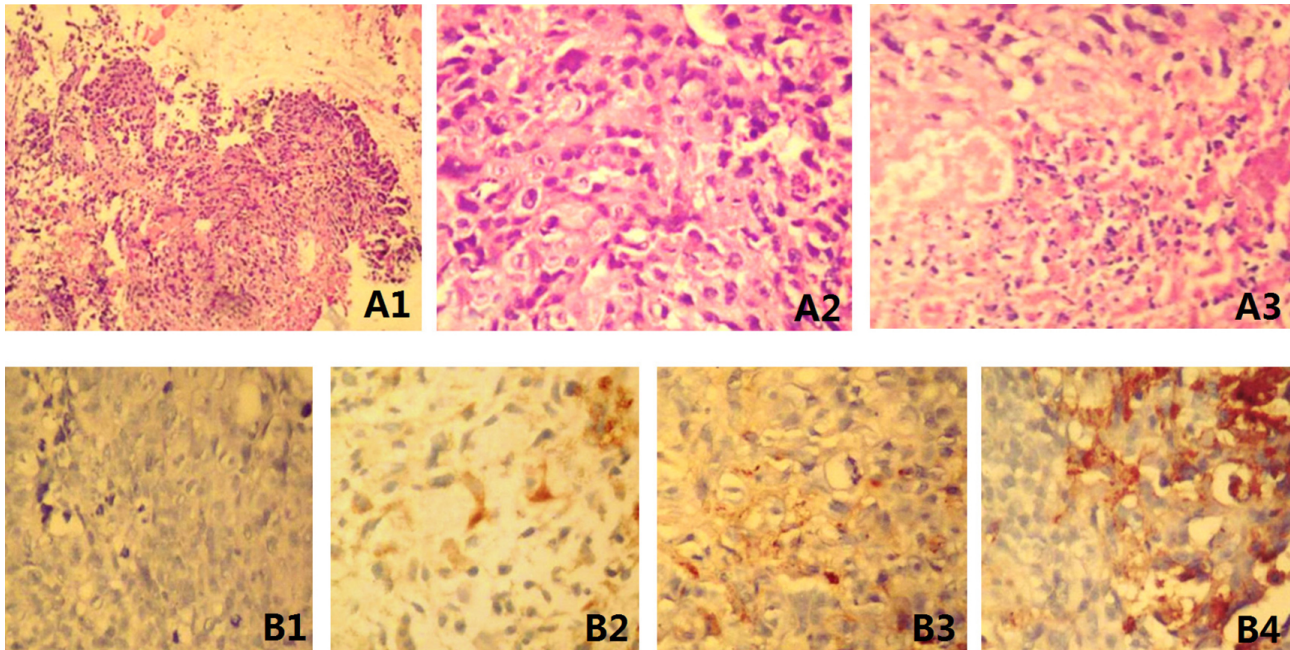


**Figure 6.** A. HE staining for transplanted tumor tissue. A1, tumor and interstitial tissue under low power lens (light microscope 100 $\times$ ); A2, jightly proliferative heteromorphic trophocytes (light microscope 400 $\times$ ); A3, hemorrhagic necrosis at the lower right corner (light microscope 400 $\times$ ). B: Immunohistochemical staining for  $\beta$ -HCG in transplanted tumor tissue (light microscope 400 $\times$ ). B1, negative expression and B2, B3, and B4, positive expression ranging from 2 to 4 points.

from 2 to 4 points, but there was no statistical difference based on inter-group comparisons (Figure 6B).

### 3.6.4 Determination of $\beta$ -HCG in serum of SCID mice

Chemiluminescence was used to analyze the content of  $\beta$ -HCG in serum. The result showed that the serum  $\beta$ -HCG of SCID mice without tumor-cell inoculation tested negative (less than 0.1 mIU/mL. Table 3 shows the values of serum  $\beta$ -HCG determined in various groups with transplanted choriocarcinoma tumor.

## 4 Discussion

Choriocarcinoma is a common malignant tumor of the female reproductive system [18-22]; chemotherapy is one of the main treatments. In recent years, seeking chemotherapeutic drugs with few toxic and side effects has become the focus of studies on antineoplastic drugs. Radix Puerariae is widely distributed in various regions of China, except Xinjiang, Qinghai, and Tibet. The monomeric compound puerarin extracted from puerarin has certain therapeutic effects on suppression and prevention of the cancer; experiments on animals have shown that it has few toxic and side effects. The preliminary result has shown that its toxic dose in rats is more than 1000 mg/kg.

**Table 3.** Values of serum  $\beta$ -HCG determined in various groups with transplanted choriocarcinoma tumors.

Group	Serum $\beta$ -HCG (mIU/ml)
Control group	89256.32 $\pm$ 6698.35
Puerarin (20 mg/kg)	38339.46 $\pm$ 2906.53*
Puerarin (40 mg/kg)	23804.83 $\pm$ 3947.61*
Puerarin (80 mg/kg)	10126.27 $\pm$ 1865.09*
5-FU (25 mg/kg)	13214.58 $\pm$ 2538.46*
Puerarin (20 mg/kg)+5-FU (25 mg/kg)	5135.62 $\pm$ 803.27*#

\* Signifies  $P < 0.05$  compared with the control group; # signifies  $P < 0.05$  compared with the monotherapy group at the same concentration.

Thus, the present study involves in-depth research on the effect of puerarin on proliferation and apoptosis of human choriocarcinoma cells and its action mechanism.

The experiment used the MTT method to detect the effect of puerarin on proliferation of the human choriocarcinoma JEG-3 cells [23-25]. MTT detection results have shown that puerarin plays a significant role in inhibiting proliferation of the human choriocarcinoma JEG-3 cells and exhibits dose- and time-dependence: the killing effect of the tumor cells will be strengthened with increasing the drug dose and action time within a certain concentration and time range.

This research has shown that the apoptosis rate rises with the increase of the drug concentration within a certain concentration range when puerarin alone is used for treating the JEG-3 cells. The apoptosis rate in the group with drug combination of puerarin (5  $\mu\text{mol/L}$ ) and 5-FU (25  $\mu\text{g/L}$ ) increased significantly compared with that in the group with monotherapy at the same concentration. Therefore, the effect of puerarin on the human choriocarcinoma JEG-3 cells was obvious from the apoptosis perspective.

Combination of puerarin and 5-FU plays a more effective role in inhibiting proliferation of the JEG-3 cells than monotherapy. Detection of apoptosis has also indicated that the apoptosis rate using the drug combination is significantly higher than that under monotherapy. The role of puerarin in inhibiting proliferation and promoting apoptosis of the human choriocarcinoma JEG-3 cells *in vitro* and the synergistic enhancement effect of puerarin in combination with 5-FU provide an experimental foundation for seeking new drugs for choriocarcinoma chemotherapy. The results have also suggested that the anti-tumor effect of puerarin may be associated with inhibiting proliferation of tumor cells and promotion apoptosis of tumor cells; its action mechanism is not strictly the same as that of 5-FU.

In the experiments, RT-PCR and Western blot have been used to detect the expression of mTOR, upstream regulatory factors AKT, and downstream regulatory factors P70S6K in terms of the mRNA level and protein level. The result has shown that with increasing puerarin concentration, the relative expression quantities of mRNA of AKT, mTOR, and P70S6K, protein, and corresponding phosphorylated protein in the JEG-3 cells are lower than those in the control group, indicating that puerarin may inhibit proliferation of human choriocarcinoma JEG-3 cells by the mTOR signaling pathway. It also indicates that the mTOR signaling pathway may become a new target site for choriocarcinoma treatment. In addition, the Western blot result indicates that with rising puerarin concentration, the expression of pro-caspase-3 in the JEG-3 cells does not change significantly, whereas the expression of cleaved-caspase-3 increases gradually and the expression of Bcl-2 decreases gradually, suggesting that the Caspase-3 and Bcl-2 families participate in the process where puerarin induces apoptosis of the JEG-3 cells.

We have successfully established the human choriocarcinoma subcutaneous transplantation tumor model using the SCID mice. The result indicates that the subcutaneously transplanted tumor of choriocarcinoma established by inoculating SCID mice with the JEG-3

cells can serve as an experimental model for screening antineoplastic drugs because it is characterized by a high tumor formation rate (100%), stable growth rate, good stability, and small difference in sizes of tumor nodules. We have observed the effect of puerarin monotherapy and combination of puerarin and 5-FU on tumor-bearing mice after the animal experimental models of SCID mouse choriocarcinoma subcutaneously transplanted tumor were successfully established. The experimental results have indicated that the final volume and weight of the transplanted tumor in the drug groups are significantly lower than that in the control group. The anti-tumor effect of the puerarin group is becoming more and more significant with the drug action time and exhibits dose dependence. In the high-dose (80 mg/kg) puerarin group, the tumor volume inhibition rate is 75.31%, and the tumor weight inhibition rate was 72.20% at the end of the experiment. Its effect is close to the anti-tumor effect of the conventional chemotherapeutic drug of 5-FU (25 mg/kg). The inhibition effect becomes more significant after combination of puerarin and 5-FU.

The electrochemical luminescence method [26-28] for detecting serum  $\beta$ -HCG is superior to radioimmunoassay and ELISA. It has been widely and clinically used.  $\beta$ -HCG is the most important index for treatment of trophocytes and follow-up visits [29, 30] and closely associated with the therapeutic effect. The experimental result has shown that the serum  $\beta$ -HCG decreases significantly after the action of drug, which further demonstrating the role of puerarin in inhibiting the transplanted tumor of the SCID mice with human choriocarcinoma.

## 5 Conclusion

In conclusion, puerarin in combination with 5-FU could inhibit proliferation and induce apoptosis of human choriocarcinoma JEG-3 cells, probably via the mTOR signaling pathway. Thus, the mTOR signaling pathway may become a new target for choriocarcinoma treatment.

**Acknowledgements:** This research is funded by Project of Incentive Funds for Guidance of Scientific and Technical Innovation in Inner Mongolia Autonomous Region (No.: 2014cztcxyd), National Natural Science Foundation of China (No.: 81260571), and Nature Science Foundation of Inner Mongolia Autonomous Region (2013MS1224).

**Conflicts of Interest:** All authors declare that they have no conflict of interest

## References

- [1] Abbasi N.Z., Zahur Z., Sheikh A.S., Khan A.A., Ahmed F., Memon K.H., et al., Testicular choriocarcinoma: diagnosed on cervical lymph node biopsy, *J. Pak. Med. Assoc.*, 2014, 63, 1544-1546.
- [2] Yazgan Y., Öncü K., Kaplan M., Tanoğlu A., Küçük I., Özari H.O., et al., Upper gastrointestinal bleeding as an initial manifestation of metastasis secondary to choriocarcinoma, *Turk. J. Gastroenterol.*, 2014, 24, 565-567.
- [3] Chen Y., Qian H., Wang H., Zhang X., Fu M., Liang X., et al., Ad-PUMA sensitizes drug-resistant choriocarcinoma cells to chemotherapeutic agents, *Gynecol. Oncol.*, 2007, 107, 505-512.
- [4] Kawamura K., Kawamura N., Okamoto N., Manabe M., Suppression of choriocarcinoma invasion and metastasis following blockade of BDNF/TrkB signaling, *Cancer Med.*, 2014, 2, 849-861.
- [5] Sorbi F., Sisti G., Pieralli A., Di Tommaso M., Livi L., Buccoliero A.M., et al., Cervicoisthmic choriocarcinoma mimicking cesarean section scar ectopic pregnancy, *J. Res. Med. Sci.*, 2014, 18, 914-917.
- [6] Dach J., Jeffrey Dach, MD: The Transition to a Natural Medicine Practice, *Altern. Ther. Health M.*, 2014, 20, 52-57.
- [7] Ni Y., Zhuang H., Kokot S., A High Performance Liquid Chromatography and Electrospray Ionization Mass Spectrometry Method for the Analysis of the Natural Medicine, *Forsythia Suspensa*, *Anal. Lett.*, 2014, 47, 102-116.
- [8] Niitsu T., Okamoto H., Iyo M., Behavioural and psychological symptoms of dementia in an Alzheimer's disease case successfully treated with natural medicine: association with gonadotropins, *Psychogeriatrics*, 2013, 13, 124-127.
- [9] Li H., Dong L., Liu Y., Wang G., Zhang L., Qiao Y., Comparison of two approaches of intestinal absorption by puerarin, *J. Pharmacol. Toxicol. Methods*, 2014, 70, 6-11.
- [10] Pignataro G., Capone D., Polichetti G., Vinciguerra A., Gentile A., Di Renzo G., et al., Neuroprotective, immunosuppressant and antineoplastic properties of mTOR inhibitors: current and emerging therapeutic options, *Curr. Opin. Pharmacol.*, 2011, 11, 378-394.
- [11] Gentzler R.D., Altman J.K., Platanius L.C., An overview of the mTOR pathway as a target in cancer therapy, *Expert Opin. Ther. Targets*, 2012, 16, 481-489.
- [12] Kim Y.J., Lee J., Song M.K., Han T., Ryu J.C., Valproic acid inhibits cell size and cell proliferation by AMPK-mediated mTOR signaling pathway in JEG-3 cells, *BioChip J.*, 2013, 7, 267-277.
- [13] Eren Y., Özata A., Determination of mutagenic and cytotoxic effects of Limonium globuliferum aqueous extracts by Allium, Ames, and MTT tests, *Rev. Bras. Farmacogn.*, 2014, 24, doi: 10.1590/0102-695X20142413322.
- [14] Morice L., Benaitreau D., Dieudonné M.N., Morvan C., Serazin V., de Mazancourt P., et al., Effets antiprolifératifs et proapoptotiques du bisphénol A dans les cellules trophoblastiques humaines JEG-3, *Immuno-Anal. Biol. Spe.*, 2012, 27, 168-176.
- [15] Xu J.T., Zhao X., Yaster M., Tao Y.X., Expression and distribution of mTOR, p70S6K, 4E-BP1, and their phosphorylated counterparts in rat dorsal root ganglion and spinal cord dorsal horn, *Brain Res.*, 2010, 1336, 46-57.
- [16] Lee D.Y., Li Y.S., Chang S.F., Zhou J., Ho H.M., Chiu J.J., et al., Oscillatory flow-induced proliferation of osteoblast-like cells is mediated by alpha vbeta3 and beta1 integrins through synergistic interactions of focal adhesion kinase and Shc with phosphatidylinositol 3-kinase and the Akt/mTOR/p70S6K pathway, *J. Biol. Chem.*, 2009, 285, 30-42.
- [17] Zheng J.H., Lu J.Q., Cheng M.J., Xu C.J., [Lung metastasis of human choriocarcinoma in mice: establishment of experimental metastatic model and its biological characteristics], *Zhonghua Fu Chan Ke Za Zhi*, 2010, 45, 519-524.
- [18] Sekine R., Hyodo M., Kojima M., Meguro Y., Suzuki A., Yokoyama T., et al., Primary hepatic choriocarcinoma in a 49-year-old man: report of a case, *World J. Gastroenterol.*, 2014, 19, 9485-9489.
- [19] Froeling F.E., Seckl M.J., Gestational Trophoblastic Tumours: An Update for 2014, *Curr. Oncol. Rep.*, 2014, 16, 408.
- [20] Berkowitz R.S., Goldstein D.P., Horowitz N.S. Management Options of Gestational Trophoblastic Disease, *Curr. Obstet. Gynecol. Rep.*, 2014, 3, 76-83.
- [21] Cole L.A., The hCG Group: the Key Molecules in Human Evolution, Human Life, and Human Death, *Curr. Obstet. Gynecol. Rep.*, 2014, 3, 91-101.
- [22] Strohl A.E., Lurain J.R., Clinical Epidemiology of Gestational Trophoblastic Disease, *Curr. Obstet. Gynecol. Rep.*, 2014, 3, 40-43.
- [23] Horn L.C., Einkenkel J., Hoehn A.K., Classification and Morphology of Gestational Trophoblastic Disease, *Curr. Obstet. Gynecol. Rep.*, 2014, 3, 44-54.
- [24] Nguyen N.M.P., Slim R., Genetics and Epigenetics of Recurrent Hydatidiform Moles: Basic Science and Genetic Counselling, *Curr. Obstet. Gynecol. Rep.*, 2014, 3, 55-64.
- [25] Shi D., Tan Z., Lu R., Yang W., Zhang Y., MicroRNA-218 inhibits the proliferation of human choriocarcinoma JEG-3 cell line by targeting Fbxw8, *Biochem. Biophys. Res. Co.*, 2014, 450, doi: 10.1016/j.bbrc.2014.06.094.
- [26] Manguso F., Bennato R., Lombardi G., Viola A., Riccio E., Picascia S., et al., P.15.6 DETERMINATION OF SERUM CORTISOL BY ECLIA UNDERESTIMATES SERUM CORTISOL SUPPRESSION IN THE PRESENCE OF PREDNISONO IN PATIENTS WITH UC. *Digest, Liver Dis.*, 2014, 46, S112.
- [27] Liu C., Chen T., Lin J., Chen H., Chen J., Lin S., et al., Evaluation of the performance of four methods for detection of hepatitis B surface antigen and their application for testing 116,455 specimens, *J. Virol. Methods*, 2014, 196, 174-178.
- [28] Yang J., Sa M., Huang M., Yang J., Xiang Z., Liu B., et al., The reference intervals for HE4, CA125 and ROMA in healthy female with electrochemiluminescence immunoassay, *Clin. Biochem.*, 2013, 46, 1705-1708.
- [29] Garrett L.D., Canine mast cell tumors: diagnosis, treatment, and prognosis, *Vet. Med. Res. Rep.*, 2014, 2014, 49-58.
- [30] Rasoulpour R.J., Terry C., LeBaron M.J., Stebbins K., Ellis-Hutchings R.G., Billington R., Mode-of-action and human relevance framework analysis for rat Leydig cell tumors associated with sulfoxaflo, *Crit. Rev. Toxicol.*, 2014, 44, 25-44.